Journal of Medicinal Chemistry

Article

pubs.acs.org/jmc

Novel Inhibitors of Neurotropic Alphavirus Replication That Improve Host Survival in a Mouse Model of Acute Viral Encephalitis

Janice A. Sindac,[‡] Bryan D. Yestrepsky,[‡] Scott J. Barraza,[‡] Kyle L. Bolduc,[‡] Pennelope K. Blakely,[∥] Richard F. Keep,[⊥] David N. Irani,[∥] David J. Miller,*[,§,#] and Scott D. Larsen*[,†,‡,#]

[†]Vahlteich Medicinal Chemistry Core and [‡]Department of Medicinal Chemistry, College of Pharmacy, [§]Departments of Internal Medicine and Microbiology and Immunology, [∥]Department of Neurology, [⊥]Departments of Neurosurgery and Neuroanatomy, University of Michigan, Ann Arbor, Michigan 48109, United States

ABSTRACT: Arboviral encephalitis is a potentially devastating human disease with no approved therapies that target virus replication. We previously discovered a novel class of thieno[3,2-*b*]pyrrole-based inhibitors active against neurotropic alphaviruses such as western equine encephalitis virus (WEEV) in cultured cells. In this report, we describe initial development of these novel antiviral compounds, including bioisosteric replacement of the 4*H*-thieno[3,2-*b*]pyrrole core with indole to improve metabolic stability and the introduction of chirality to assess target enantioselectivity. Selected modifications enhanced antiviral activity while maintaining low cytotoxicity, increased stability to microsomal metabolism, and also revealed striking enantiospecific activity in cultured cells. Furthermore, we demonstrate improved outcomes (both symptoms and survival) following treatment with indole analogue **9h** (CCG-203926) in an in vivo mouse model of alphaviral encephalitis that closely correlate with the enantiospecific in vitro antiviral activity. These results represent a substantial advancement in the early preclinical development of a promising class of novel antiviral drugs against virulent neurotropic alphaviruses.

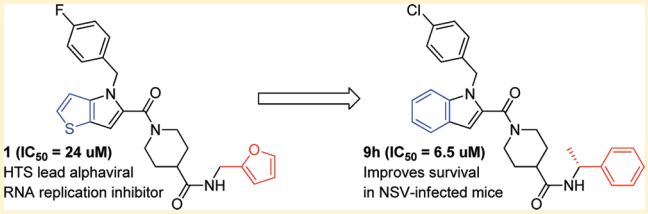

INTRODUCTION

Infections caused by insect-borne viruses (arboviruses) represent some of the most dramatic examples of disease re-emergence throughout the world.[1] This is due in part to the significant growth in urban centers in the latter half of the 20th century, which has produced societal conditions that can greatly facilitate arbovirus epidemics. One particularly frightening public health scenario is the recent expansion of specific arboviral diseases outside of their historical geographic boundaries.[2−4] Furthermore, there is the potential for an intentional introduction of a virulent arbovirus into the environment or select communities. This has prompted public health authorities to list numerous arboviruses as high priority biodefense pathogens, particularly those that infect the central nervous system (CNS) and cause acute encephalitis.[5] This is due in part to numerous characteristics that make them potential biological weapons: (i) high clinical morbidity and mortality, (ii) potential for aerosol transmission, (iii) lack of effective countermeasures for disease prevention or control, (iv) public anxiety elicited by CNS infections, (v) ease with which large volumes of infectious materials can be produced, and (vi) potential for malicious introduction of foreign genes designed to increase virulence.[6,7] The near complete absence of effective drugs to treat neurotropic arbovirus infections highlights the need for novel approaches to identify and develop antiviral agents for these potentially devastating diseases, but research to date in this area has been sparse.[8−11]

We recently reported the identification of a class of small molecules that inhibit RNA replication of the neurotropic alphavirus western equine encephalitis virus (WEEV).[12] The lead compound **1** (CCG-32091, Figure 1), discovered via high-throughput screening (HTS) in the University of Michigan Center for Chemical Genomics (CCG), possessed modest potency with low cytotoxicity. Furthermore, initial structure−activity relationship (SAR) analysis elucidated with available library and commercial analogues was encouraging, with small changes in structure resulting in large changes in activity.

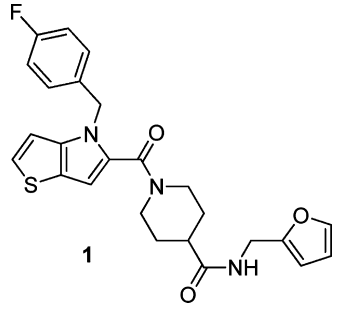

Figure 1. Structure of HTS lead **1**.

We initiated a medicinal chemistry program around **1** with two goals in mind: (1) to identify the macromolecular target and (2) to achieve proof-of-concept activity in an animal model of alphaviral encephalitis. With regard to the first goal, we

Received: February 16, 2012
Published: March 19, 2012

designed initial analogues of **1** bearing chiral centers to determine if eudismic ratios were detectable, which would establish confidence that our lead was acting through binding to a chiral macromolecule. With regard to in vivo efficacy, we needed to improve the modest potency of the lead (IC_{50} = 24 μM) while maintaining low cytotoxicity, and we were concerned about the potential metabolic instability of the electron-rich 4*H*-thieno[3,2-*b*]pyrrole ring.[13] Thienopyrrole is a classic bioisostere for indole,[14,15] so the feasibility of replacing the central bicyclic template of **1** with indole was also investigated.

CHEMISTRY

The preparation of new thieno[3,2-*b*]pyrrole analogues is summarized in Scheme 1. Methyl ester **2** was *N*-alkylated

Scheme 1. Preparation of Thieno[3,2-*b*]pyrrole Analogues of 1[a]

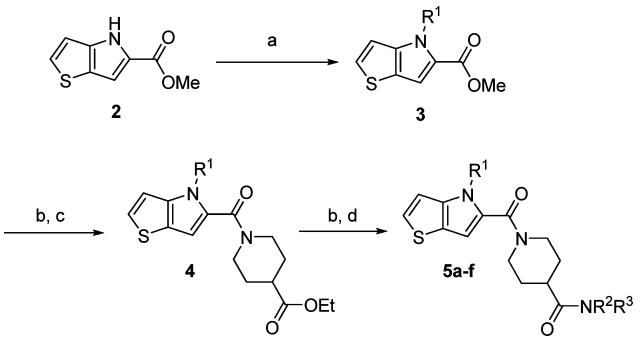

[a]Reagents and conditions: (a) K_2CO_3, DMF, R^1Cl or Ph_3P, DIAD, R^1OH, THF; (b) KOH, aq EtOH, 40 °C; (c) ethyl isonipecotate, EDC, HOBt, DIEA, DCM, RT; (d) HNR^2R^3, EDC, HOBt, DIEA, RT.

under basic conditions with various benzyl chlorides or under Mitsunobu conditions[16] with benzyl alcohols to afford thieno-[3,2-*b*]pyrroles **3**. Following saponification of the ester, EDC-mediated amidation with ethyl isonipecotate provided esters **4**. Final analogues **5** were obtained after a second saponification and EDC-mediated amidation with various amines. Indole analogues **9** were prepared in an analogous fashion starting with ethyl indole-2-carboxylate (Scheme 2).

Scheme 2. Preparation of Indole Analogues of 1[a]

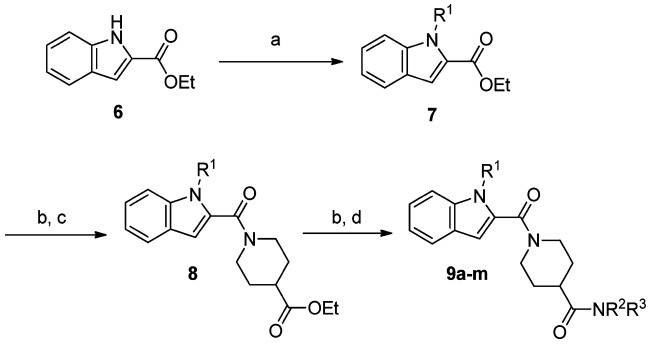

[a]Reagents and conditions: (a) K_2CO_3, DMF, R^1Cl, 60 °C; (b) LiOH, aq THF, 60 °C; (c) ethyl isonipecotate, EDC, HOBt, DIEA, DMF, RT; (d) HNR^2R^3, EDC, HOBt, DIEA, RT.

RESULTS AND DISCUSSION

WEEV Replicon SAR. All new analogues were evaluated with the cell-based replicon assay initially developed for the HTS, in which the majority of the WEEV structural genes are replaced with the firefly luciferase gene as a reporter for viral RNA replication[12] and with an MTT assay to evaluate their effects on cell viability (Table 1). We limited our initial SAR investigation to thieno[3,2-*b*]pyrroles and indoles that incorporated R^1 groups that were derivatives of benzyl, based on the favorable activity exhibited by such analogues in our previous work.[12] After replacing the 2-furanylmethyl amide of **1** with equipotent benzyl amide (**5a**) to improve predicted stability to oxidative metabolism, an initial increase in potency was realized by replacing the 4-fluorobenzyl at R^1 with 4-chlorobenzyl (**5b**). The impact of adding chirality at two different positions was evaluated with analogues **5c**–**5f**. Interestingly, a eudismic ratio was established at each position but was apparently larger on the benzyl amide (**5c** vs **5d**) than the pyrrole N-substituent (**5e** vs **5f**). *In the absence of a known molecular target, these results are highly significant in that they are strong evidence that our series is binding to a chiral macromolecule.*

Remaining SAR was elucidated on the bioisosteric indole template **9**. Importantly, the prototype analogue **9a** showed no loss in activity in the replicon assay versus the corresponding thieno[3,2-*b*]pyrrole **5a** (Table 1). Interestingly, replacing the 4-fluorobenzyl with 4-chlorobenzyl (**9b**) did not improve activity as in the thieno[3,2-*b*]pyrrole series. Moving the benzylamide moiety from the 4-position of the piperidine to the 3-position (**9c**) was detrimental to activity, as we observed previously in the thienopyrrole series.[12] Shortening the benzylamide by one carbon (**9d**) resulted in total loss of activity, while lengthening it to 2-phenylethylamide (**9e**) maintained activity but introduced some cytotoxicity. Appending a *para*-methyl group to the phenylethylamide (**9f**), however, provided a significant boost in activity, improving the therapeutic index (CC_{50}/IC_{50}) to 14. As anticipated, incorporating chirality into the benzylamide established the same eudismic ratio as observed with the thieno-[3,2-*b*]pyrroles, with the (*R*)-enantiomer **9h** having superior activity over (*S*)-enantiomer **9g**. These results strongly suggest that the indoles are binding in a very similar manner to the thieno[3,2-*b*]pyrroles. Final SAR in the benzyl amide series consisted of 4-methoxy (**9i**) and 3-chloro (**9j**) substitution, the former leading to complete loss of activity. One simple alkyl amide (**9k**) evaluated in this initial SAR survey maintained activity but at the cost of increased cytotoxicity. A preliminary examination of heterocycles was more encouraging, with 4-pyridylmethyl amide **9l** demonstrating a significant boost in activity over the benzyl amide **9b** with no apparent increase in cytotoxicity. The closely related 3-pyridylmethyl amide **9m** was somewhat less active.

Included in Table 1 are calculated partition coefficients (ClogP), a common estimator of lipophilicity. It is quite possible that some of the observed differences in replicon inhibition were due to simple changes in this parameter, as it is generally accepted that higher lipophilicity results in greater cell permeability.[17] For example, some or all of the improved activity of phenethyl amide **9f** vs benzyl amide **9b** could simply be due to its higher lipophilicity and thus expected higher passive permeability. However, it is conversely very likely that the improved potency of 4-pyridylmethyl amide **9l** vs **9b** is a reflection of better intrinsic activity rather than passive permeability due to its significantly lower ClogP. Similarly, the eudismic ratios observed for the three

dx.doi.org/10.1021/jm300214e | J. Med. Chem. 2012, 55, 3535–3545

Table 1. WEEV Replicon and Physical Property Data for New Analogues (Schemes 1 and 2)

compd	R^1	NR^2R^3	IC_{50} (μM)[a]	CC_{50} (μM)[b]	CC_{50}/IC_{50}	ClogP[c]	Log P_{eff}[d]	MLM $T_{1/2}$ (min)[e]
1	4-F-Ph-CH_2	$NHCH_2$furan-2-ylNH	24.4 ± 6.9	>100	>4.1	3.05		
5a	4-F-Ph-CH_2	$NHCH_2$Ph	25.4 ± 7.3	>100	>3.9	3.88		
5b	4-Cl-Ph-CH_2	$NHCH_2$Ph	10.1 ± 2.6	>100	>9.9	4.45	−3.6 ± 0. 01	1.7 ± 1.7
5c	4-F-Ph-CH_2	(*S*)-NHCH(CH_3)Ph	>100	>100		4.76		
5d	4-F-Ph-CH_2	(*R*)-NHCH(CH_3)Ph	8.3 ± 1.3	93.4	11	4.76		
5e	(*R*)-4-F-PhCH(CH_3)	$NHCH_2$Ph	18.4 ± 4.7	>100	>5.4	4.04		
5f	(*S*)-4-F-PhCH(CH_3)	$NHCH_2$Ph	>100	>100		4.04		
9a	4-F-Ph-CH_2	$NHCH_2$Ph	14.8 ± 5.8	>100	>6.7	3.98		
9b	4-Cl-Ph-CH_2	$NHCH_2$Ph	15.5 ± 5.6	>100	>6.5	4.55	−3.6 ± 0.03	7.3 ± 3.9
9c	4-Cl-Ph-CH_2	$NHCH_2$Ph[f]	30.6 ± 7.3	>100	>3.3	5.71		
9d	4-Cl-Ph-CH_2	NHPh	>50	ND[g]		4.92		
9e	4-Cl-Ph-CH_2	$NHCH_2CH_2$Ph	15.2 ± 9.3	62.1	4.1	4.62		
9f	4-Cl-Ph-CH_2	$NHCH_2CH_2$(4-Me-Ph)	5.5 ± 2.2	75.2	14	5.12	−3.9 ± 0.11	
9g	4-Cl-Ph-CH_2	(*S*)-NHCH(CH_3)Ph	>100	>100		4.86		
9h	4-Cl-Ph-CH_2	(*R*)-NHCH(CH_3)Ph	6.5 ± 1.5	89.9	14	4.86	−3.6 ± 0.03	31 ± 7.1
9i	4-Cl-Ph-CH_2	$NHCH_2$(4-MeO-Ph)	>50	ND		4.47		
9j	4-Cl-Ph-CH_2	$NHCH_2$(3-Cl-Ph)	15.3 ± 9.0	>100	>6.5	5.26		
9k	4-Cl-Ph-CH_2	*N*-piperidinyl	9.2 ± 2.8	51.7	5.6	3.58		
9l	4-Cl-Ph-CH_2	$NHCH_2$pyridin-4-yl	6.8 ± 1.7	>100	>14	3.05	−3.7 ± 0.17	
9m	4-Cl-Ph-CH_2	$NHCH_2$pyridin-3-yl	11.4 ± 0.4	>100	>8.7	3.05		

[a]Inhibition of luciferase expression in the WEEV replicon assay. Ribavirin (positive control) has an IC_{50} in this assay of 16 μM. [b]Cell viability as determined by inhibition of mitochondrial reduction of MTT. [c]Calculated logP (ChemBioDraw Ultra 11.0). [d]Log of effective permeability (cm/s) as determined by PAMPA Explorer (pION). [e]Half-life in mouse liver microsome incubations. [f]The amide $CONHCH_2Ph$ is bonded to the 3-position of the piperidine instead of the 4-position. [g]ND: not determined.

pairs of enantiomers likely reflect actual differences in intrinsic activity because of their identical ClogPs.

In this regard, we also evaluated selected analogues in the parallel artificial membrane permeability assay (PAMPA) as a more direct estimate of passive permeability (Table 1).[18] The most important conclusion from these studies is that as a class the analogues are predicted to have medium to high passive cell permeability ($P_{eff} \geq 10^{-4}$ cm/s), a critical requirement for compounds to be active in the CNS. It is also clear that among the analogues tested there was not a wide variation in permeability, even when lipophilicity was reduced (**9l**), which suggests that the series will have some flexibility for structural modification without loss of permeability.

In Vitro Antiviral Assays. Four analogues were selected for advancement to in vitro infection studies: the prototype thieno[3,2-*b*]pyrrole **5b** and indole **9b** analogues, along with the indole enantiomers **9g** and **9h**. We wished to directly compare the effectiveness of the two heterocyclic templates against live virus and to assess whether the indole enantiomers had antiviral activity that correlated with activity in the replicon assay.

We measured antiviral activity using two complementary assays in cultured neuronal cells: reduction in cytopathic effect (CPE) and extracellular virus titers (Figure 2). Alphaviruses such as WEEV and the related neuroadapted Sindbis virus (NSV) are highly cytolytic to cultured cells, due in part to vigorous replication and virion production, such that antiviral compounds are predicted to increase cell viability and decrease virus titers after infection. Both the thieno[3,2-*b*]pyrrole **5b** and indole **9b** analogues, as well as the indole enantiomer **9h** that was active in the replicon inhibition assay (see Table 1), increased cell viability by 1.5−2-fold after either WEEV or NSV infection (Figure 2A). In contrast, the indole enantiomer **9g**, which was inactive in the replicon inhibition assay, was unable

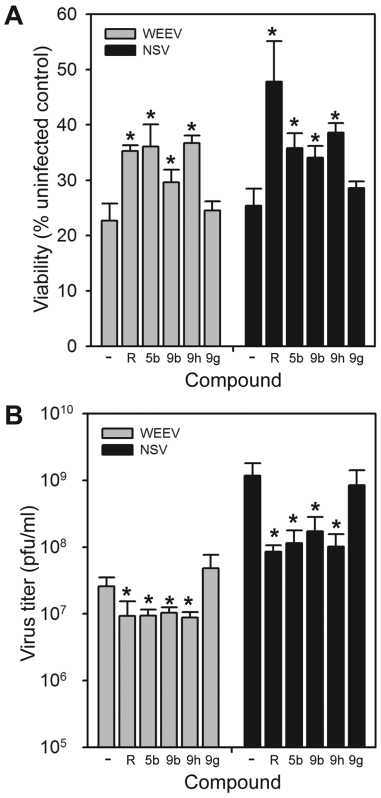

Figure 2. Neuronal cell infection studies. Cultured human BE(2)-C neuronal cells were simultaneously infected with WEEV or NSV and incubated with the indicated compounds at a final concentration of 25 μM. Cell viability (A) and virus titers (B) were determined 24 h post-infection by MTT and plaque assays, respectively. Ribavirin (R) was used as the positive control for both assays. *$p < 0.05$ compared to DMSO (—) controls.

dx.doi.org/10.1021/jm300214e | *J. Med. Chem.* 2012, 55, 3535−3545

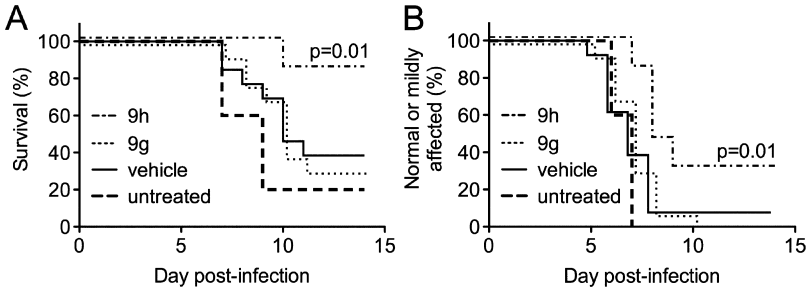

Figure 3. Clinical effects of the indole enantiomers, **9g** and **9h**, in mice with acute NSV encephalomyelitis. Cohorts of infected mice (n = 13/group) were otherwise not manipulated or were treated with **9g** or **9h** (30 mg/kg/dose) or with a vehicle control by intraperitoneal injection every 12 h beginning 12 h after virus challenge and continuing for the next 7 days. (A) Survival differences between drug- and vehicle-treated animals were measured using a log-rank (Mantel−Cox) test. (B) Similarly, the proportion of mice that either developed mild or no hind limb paralysis following NSV challenge was determined in each group, and differences between drug- and vehicle-treated animals determined by a log-rank (Mantel−Cox) test.

to rescue virus-induced CPE. We obtained consistent results when we measured virion production via plaque assays, where the thieno[3,2-*b*]pyrrole **5b**, the indole **9b** analogue, and the indole enantiomer **9h** all significantly reduced both WEEV and NSV titers, whereas the indole enantiomer **9g** was inactive in this assay (Figure 2B). These antiviral assay results correlated with the replicon inhibition studies (Table 1) and support the conclusion that chirality at the benzylamide position is a major determinant of compound activity. Moreover, the antiviral effects of **5b**, **9b**, and **9h** were comparable to those of ribavirin, an established broad spectrum antiviral agent used as a positive control.

Metabolic Stability. Because the new indole template **9** was selected in part based on its expected higher resistance to oxidative metabolism, we also undertook a preliminary evaluation of the stability of prototypes **5b** and **9b** to metabolism by mouse liver microsomes (MLMs). Indole **9b** was found to have a longer half-life than the corresponding thieno[3,2-*b*]pyrrole **5b** (7.3 min vs 1.7 min, Table 1), suggesting that the new indole series should have greater potential for in vivo efficacy. On the basis of its promising antiviral activity, we also evaluated α-methyl benzylamide analogue **9h**. Interestingly, the stability of **9h** to metabolism by MLMs is significantly higher than prototype indole benzylamide **9b** ($T_{1/2}$ = 31 min vs 7.3 min, Table 1), suggesting that the benzyl amide CH_2 may be a major site of oxidative metabolism that is being sterically shielded by the methyl group.

In Vivo Infection Studies. We selected the indole enantiomers **9g** and **9h** for initial in vivo testing. Compound **9h** offered favorable antiviral activity, relatively low cytotoxicity, and good stability to microsomal metabolism, while **9g** provided an ideal negative control as a closely related but inactive enantiomer. We chose NSV as our initial in vivo model due to the lower biosafety requirements for this pathogen (BSL2 containment) compared to highly virulent WEEV (BSL3 containment). Without treatment, direct intracerebral injection of NSV causes hind limb paralysis and death in weanling mice. Pilot survival assays using **9h** at doses of 10 mg/kg and 30 mg/kg suggested that the higher concentration was more effective (data not shown). In larger experimental cohorts, mice treated with **9h** at a dose of 30 mg/kg twice daily beginning 12 h after viral challenge and continuing for a 7-day period (that reflects the interval of peak viral replication and clearance) were significantly protected from lethal NSV infection compared to animals that were otherwise untreated, that received a vehicle control, or that were given **9g** at the identical concentration (Figure 3A). Importantly, treatment with **9h** also conferred benefit against the development of severe hind limb paralysis prior to death (Figure 3B), a characteristic feature of NSV-induced disease that follows intracerebral challenge.[19,20]

To investigate the effects of **9g** and **9h** on virus replication in vivo, the amount of infectious NSV present directly in the CNS was measured early (1−4 days) after infection, when titers peak and then begin to wane as antiviral host immunity is activated. Plaque titration assays showed that viral titers were lower in the brains of mice receiving **9h** compared to **9g** or a vehicle control, achieving statistical significance on day 3 (Figure 4A). A similar

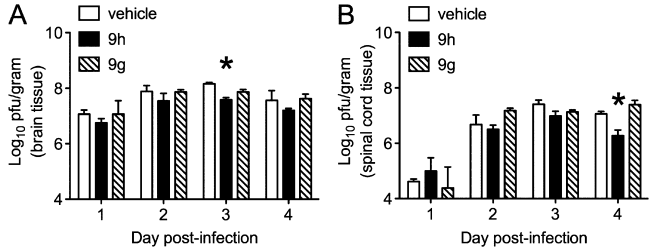

Figure 4. Virological effects of the indole enantiomers, **9g** and **9h**, in mice with acute NSV encephalomyelitis. Cohorts of NSV-infected mice were treated with **9g** or **9h** (30 mg/kg/dose) or with a vehicle control by intraperitoneal injection every 12 h beginning 12 h after virus challenge. At 24 h intervals, viral titers were measured in quadruplicate brain (A) and spinal cord (B) tissue samples from each group by plaque titration assay. Statistical differences (*p < 0.05) in tissue viral loads were determined by an unpaired Student's t-test compared to vehicle-treated controls.

extent of viral inhibition was also observed in the spinal cords of NSV-infected mice (Figure 4B). Prior studies have shown that reducing CNS viral titers by a log are associated with improved disease outcome after NSV infection.[19,20]

To determine the extent to which clinical protection correlated with enhanced neuronal survival, an established fluorojade labeling method was employed. In the hippocampus, where many neurons are infected by NSV, treatment with **9h** led to reduced neuronal injury compared to mice that were given either **9g** or a vehicle control (Figure 5B). In these assays, the Nissl substance was stained to enumerate hippocampal neurons and the proportion of these cells that were also fluorojade-positive was counted by fluorescence microscopy (example shown in Figure 5A). In the spinal cord, silver staining was used to label motor neuron axons in lumbar ventral nerve roots (Figure 6A), and the density of preserved axons following treatment with **9h** showed enhanced cell survival compared to

dx.doi.org/10.1021/jm300214e | J. Med. Chem. 2012, 55, 3535−3545

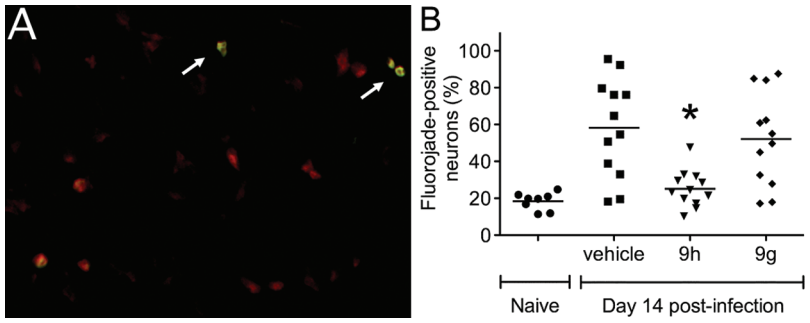

Figure 5. Effects of the indole enantiomers, **9g** and **9h**, on neuronal survival in the brains of NSV-infected mice. The anatomically defined hippocampus, a site of heavy NSV infection, was chosen for further study. (A) Representative fluorojade staining of damaged hippocampal neurons in the brains of NSV-infected mice. NisslRed was first used to label neurons in sections through the hippocampus, while fluorojade staining (arrows) was then performed to identify those cells undergoing active degeneration. (B) The proportion of fluorojade-positive hippocampal neurons was determined in quadruplicate slides prepared from 3 mice in each group. Statistical differences (*$p < 0.05$) in the number of labeled (injured) neurons were determined by an unpaired Student's *t*-test compared to vehicle-treated control animals.

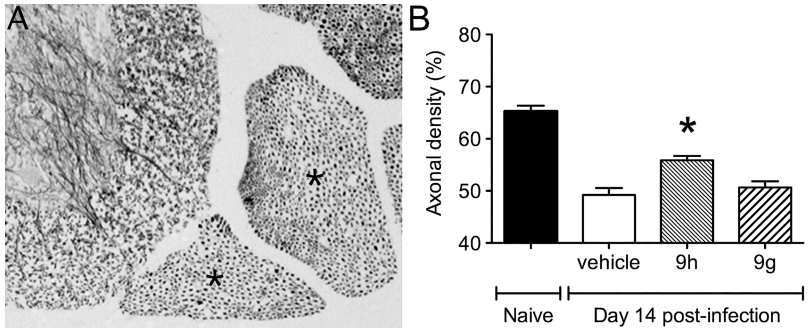

Figure 6. Effects of the indole enantiomers, **9g** and **9h**, on neuronal survival in the spinal cords of NSV-infected mice. Silver staining of tissue sections prepared from the lumbar spinal column was used to identify the ventral nerve roots and the motor neuron axons they carry. (A) A representative specimen from an uninfected animal is shown, with the L4 and L5 ventral nerve roots identified (marked with *). (B) Quantification of axonal density in these lumbar ventral nerve roots shows relative neuronal sparing in **9h**-treated animals compared to vehicle- or **9g**-treated controls. Statistical differences (*$p < 0.05$) were determined using unpaired Student's *t*-tests.

mice given **9g** or a vehicle control (Figure 6B). Taken together, these data show that **9h** exerts an antiviral effect within the CNS of NSV-infected mice, causing enhanced neuronal survival that leads to improved disease outcome.

Successful antiviral therapy in animal models of acute alphavirus encephalitis has only been accomplished in a few settings. In newborn mice, *seco*-pregnane steroids delayed mortality when given within 4 h of viral challenge but did not alter overall survival.[21] In weanling mice infected intranasally with a vaccine strain of Venezuelan equine encephalitis virus (VEEV), (−)-carbodine improved outcome when initiated up to 4 days after viral challenge while lowering peak CNS viral titers by a half-log.[22] The same drug showed no benefit following wild-type VEEV challenge. While of relatively modest clinical utility, these studies highlight the fact that successful compounds do not have to exert dramatic antiviral effects within the CNS to exert protective effects. Future studies will be aimed at broadening the window of effectiveness from the time of viral challenge and synergizing with unrelated treatments known to exert more direct neuroprotective effects.

CONCLUSIONS

In summary, our initial medicinal chemistry efforts have been successful at improving both the potency and metabolic stability of lead alphavirus RNA replication inhibitor **1**. Furthermore, we have demonstrated that the as yet unidentified molecular target exhibits a significant level of enantioselectivity, suggesting that it is a chiral macromolecule. Importantly, we have established that an analogue (**9h**, CCG-203926) with only modest potency is capable of improving outcomes, both symptoms and survival, in a mouse model of alphavirus infection, and that the observed protective effects correlate with both in vitro and in vivo antiviral activity, and with the extent of neuronal protection from viral damage. Current studies in our laboratories are aimed at further improving the potency of this new class of indole-based antiviral agents. We also intend to evaluate their efficacy in mouse models of WEEV infection, with results to be reported in due course.

EXPERIMENTAL SECTION

General Synthetic Procedures. All reagents were used as received from commercial sources unless otherwise noted. ^{1}H and ^{13}C spectra were obtained in DMSO-d_6 or $CDCl_3$ at room temperature, unless otherwise noted, on a Varian Inova 400 MHz, Varian Inova 500 MHz, or Bruker Avance DRX 500 instruments. Chemical shifts for the ^{1}H NMR and ^{13}C NMR spectra were recorded in parts per million (ppm) on the δ scale from an internal standard of residual tetramethylsilane (0 ppm). Mass spectroscopy data were obtained on a Waters Corporation LCT. Purities of final compounds used for biological testing were determined by HPLC and were ≥95% unless reported otherwise. HPLC retention times were recorded in minutes (min) using an Agilent 1100 series with an Agilent Zorbax Eclipse Plus−C18 column and a 10−90% acetonitrile/water over 13 min gradient (gradient A). Combustion analyses (CHN) were performed by Robertson Microlit Laboratories (Madison, NJ). Solvent abbreviations used: MeOH (methanol), DCM (dichloromethane), EA

dx.doi.org/10.1021/jm300214e | J. Med. Chem. 2012, 55, 3535−3545

(ethyl acetate), hex (hexanes), DMSO (dimethylsulfoxide), DMF (dimethylformamide), H_2O (water), THF (tetrahydrofuran). Reagent abbreviations used: DIAD (diisopropyl diazodicarboxylate), HOBt (1-hydroxy-1,2,3-benzotriazole), EDC (*N*-(3-dimethylaminopropyl)-*N*′-ethylcarbodiimide hydrochloride), DIEA (diisopropylethylamine), PPh_3 (triphenylphosphine), $MgSO_4$ (magnesium sulfate), $NaHCO_3$ (sodium bicarbonate), NH_4Cl (ammonium chloride), K_2HCO_3 (potassium bicarbonate), K_2CO_3 (potassium carbonate), KOH (potassium hydroxide), and HCl (hydrogen chloride). Assay abbreviations: LUC(luciferase), MTT ((3-(4,5-dimethylthiazol-2-yl)-2,5-diphenyltetrazolium bromide.

*Methyl 4H-Thieno[3,2-b]pyrrole-5-carboxylate (**2**).* 4*H*-Thieno[3,2-*b*]pyrrole-5-carboxylic acid (200 mg, 1.20 mmol) was dissolved in DMF (2.4 mL) and cooled to 0 °C in an ice bath. To this solution were added $KHCO_3$ (132 mg, 1.32 mmol) and iodomethane (150 μL, 2.40 mmol). The reaction was allowed to warm to RT and stirrred for 16 h. The reaction was diluted with H_2O (∼15 mL), causing the precipitation of a light-tan solid. The precipitate was isolated via vacuum filtration and washed with H_2O, yielding compound **2** (178 mg, 78% yield). TLC R_f (10% MeOH:DCM): 0.9. ^{1}H NMR ($CDCl_3$, 500 MHz): δ (ppm) 9.15 (bs, 1H), 7.36 (d, *J* = 5.4 Hz, 1H), 7.16 (d, *J* = 1.4 Hz, 1H), 6.99 (d, *J* = 5.4 Hz, 1H), 3.93 (s, 3H).

*Methyl N-(4-Fluoro)benzyl-4H-thieno[3,2-b]pyrrole Carboxylate (**3a**).* To a stirred solution of **2** (200 mg, 1.10 mmol) in 18 mL of DMF at 60 °C were added finely powdered K_2CO_3 (304 mg, 2.20 mmol) and 4-fluorobenzyl chloride (264 uL, 2.20 mmol). The reaction mixture was allowed to stir 18 h and monitored by TLC. The reaction mixture was diluted with ∼30 mL of H_2O and extracted with ethyl acetate (3 × 10 mL). The organic layer was washed with satd aq $NaHCO_3$, satd aq NH_4Cl, and brine. The organic layer was dried over $MgSO_4$, concentrated in vacuo, and purified via 40 g Biotage CombiFlash silica column (2:1 hexane:ethyl acetate), affording **3a** (221 mg, 69% yield) as a viscous brown oil. TLC R_f (33% EA:hexane): 0.81. ^{1}H NMR ($CDCl_3$, 500 MHz): δ (ppm) 7.40 (d, *J* = 5.4 Hz, 2H), 7.14 (m, 2H), 6.99 (t, *J* = 8.7 Hz, 2H), 6.88 (d, *J* = 5.4 Hz, 1H), 5.74 (s, 2H), 3.86 (s, 3H).

*(R)-Methyl 4-(1-(4-Fluorophenyl)ethyl)-4H-thieno[3,2-b]pyrrole-5-carboxylate (**3e**).* Compound **2** (100 mg, 0.551 mmol), PPh_3 (289 mg, 1.10 mmol), and (*S*)-1-(4-fluorophenyl)ethanol (104 μL, 1.10 mmol) were combined in 1.8 mL of anhydrous THF at 0 °C. DIAD (212 μL, 1.10 mmol) was then added dropwise. The reaction mixture was stirred at 0 °C for 1 h, then allowed to warm to RT for an additional 12 h. The solvent was removed in vacuo, leaving a viscous black liquid that was purified via Biotage (10 g silica column, 5:1 hexanes:ethyl acetate) to yield compound **3e** (104 mg, 62% yield) as a clear oil. TLC R_f (20% EA:hex): 0.65. ^{1}H NMR ($CDCl_3$, 500 MHz): δ (ppm) 7.25 (m, 3H), 7.19 (d, *J* = 5.4 Hz, 1H), 7.02 (t, *J* = 8.7 Hz, 2H), 6.97 (q, *J* = 6.9 Hz, 1H), 6.45 (d, *J* = 5.4 Hz, 1H), 3.90 (s, 3H), 1.91 (d, *J* = 6.9 Hz, 3H).

*(S)-Methyl 4-(1-(4-Fluorophenyl)ethyl)-4H-thieno[3,2-b]pyrrole-5-carboxylate (**3f**).* Prepared in the same manner as compound **3e** starting with (*R*)-1-(4-fluorophenyl)ethanol. TLC R_f (20% EA:hex): 0.65. ^{1}H NMR ($CDCl_3$, 500 MHz): δ (ppm) 7.25 (m, 3H), 7.19 (d, *J* = 5.4 Hz, 1H), 7.02 (t, *J* = 8.7 Hz, 2H), 6.97 (quart, *J* = 6.9 Hz, 1H), 6.45 (d, *J* = 5.4 Hz, 1H), 3.90 (s, 3H), 1.91 (d, *J* = 6.9 Hz, 3H).

*Ethyl 1-(4-(4-Fluorobenzyl)-4H-thieno[3,2-b]pyrrole-5-carbonyl)-piperidine-4-carboxylate (**4a**).* Compound **3a** (179 mg, 0.619 mmol) and KOH (118 mg, 2.11 mmol) were dissolved in a 3:1 EtOH:H_2O solution (6 mL). The mixture was heated to 40 °C and allowed to stir for 16 h. The reaction was judged complete by TLC. Reaction was quenched by the addition of 1N HCl (30 mL), causing immediate precipitation of a white solid. Solid was collected via vacuum filtration and washed with H_2O. Drying in vacuo yielded the carboxylic acid as a white powder (147 mg, 86% yield). The isolated carboxylic acid (391 mg, 1.42 mmol) was dissolved in DCM (14 mL), to which EDC (326 mg, 1.70 mmol), 1-hydroxybenzotriazole (230 mg, 1.70 mmol), and DIEA (371 μL, 2.13 mmol) were added. The solution was allowed to stir at RT for 30 min, at which point ethyl isonipecotate (328 μL, 2.13 mmol) was added. The reaction was allowed to stir at RT for 16 h. The reaction was then diluted with additional DCM (25 mL) and washed in a separatory funnel sequentially with satd aq NH_4Cl, H_2O, and brine. The organic layer was dried over $MgSO_4$ and purified via Biotage silica column (10 g, 100% hexane to 33% EA:hex elution), yielding **4a** as a light-brown oil (49 mg, 80% yield). TLC R_f (1:1 hex:EA): 0.60. ^{1}H NMR ($CDCl_3$, 500 MHz): δ (ppm) 7.21 (d, *J* = 5.3 Hz, 1H), 7.15 (dd, *J* = 5.5, 8.5 Hz, 2H), 6.97 (t, *J* = 8.5 Hz, 2H), 6.91 (d, *J* = 5.4 Hz, 1H), 6.58 (s, 1H), 5.45 (s, 2H), 4.36−4.26 (m, 2H), 4.17 (quart, *J* = 7.2 Hz, 2H), 3.08−2.97 (m, 2H), 2.50 (quint, *J* = 3.7 Hz, 1H), 1.92−1.80 (bm, 2H), 1.54−1.35 (bm, 2H), 1.29 (t, *J* = 7.2 Hz, 3H).

*(R)-Ethyl 1-(4-(1-(4-Fluorophenyl)ethyl)-4H-thieno[3,2-b]pyrrole-5-carbonyl)piperidine-4-carboxylate (**4e**).* Synthesized in the same manner as compound **4a**. TLC R_f (33% EA:hex): 0.45. ^{1}H NMR ($CDCl_3$, 500 MHz): δ (ppm) 7.21 (d, *J* = 5.3 Hz, 1H), 7.15 (dd, *J* = 5.5, 8.5 Hz, 2H), 6.97 (t, *J* = 8.5 Hz, 2H), 6.91 (d, *J* = 5.4 Hz, 1H), 6.58 (s, 1H), 6.22 (q, 6.4 Hz, 1H), 4.36−4.26 (m, 2H), 4.17 (quart, *J* = 7.2 Hz, 2H), 3.08−2.97 (m, 2H), 2.50 (quint, *J* = 3.7 Hz, 1H), 1.93 (d, 6.4 Hz, 3H), 1.92−1.80 (bm, 2H), 1.54−1.35 (bm, 2H), 1.29 (t, *J* = 7.2 Hz, 3H).

*(S)-Ethyl 1-(4-(1-(4-Fluorophenyl)ethyl)-4H-thieno[3,2-b]pyrrole-5-carbonyl)piperidine-4-carboxylate (**4f**).* Synthesized in the same manner as compound **4a**. TLC R_f (33% EA:hex): 0.45. ^{1}H NMR ($CDCl_3$, 500 MHz): δ (ppm) 7.21 (d, *J* = 5.3 Hz, 1H), 7.15 (dd, *J* = 5.5, 8.5 Hz, 2H), 6.97 (t, *J* = 8.5 Hz, 2H), 6.91 (d, *J* = 5.4 Hz, 1H), 6.58 (s, 1H), 6.22 (q, 6.4 Hz, 1H), 4.36−4.26 (m, 2H), 4.17 (quart, *J* = 7.2 Hz, 2H), 3.08−2.97 (m, 2H), 2.50 (quint, *J* = 3.7 Hz, 1H), 1.93 (d, 6.4 Hz, 3H), 1.92−1.80 (bm, 2H), 1.54−1.35 (bm, 2H), 1.29 (t, *J* = 7.2 Hz, 3H).

General Procedure A for Generating Analogues 5a−f from 4. Compound **4a** (333 mg, 0.804 mmol) and KOH (158 mg, 2.82 mmol) were dissolved in 3:1 EtOH:H_2O solution (8 mL). The mixture was heated to 40 °C and allowed to stir for 16 h. The reaction was judged complete by TLC monitoring and was quenched by the addition of 1N HCl (40 mL), causing immediate precipitation of a white solid. The aqueous suspension was extracted 3× with ethyl acetate (3× 15 mL) and then washed with H_2O and brine (20 mL). The organic layer was dried over $MgSO_4$ and concentrated in vacuo to a light-brown oily solid (287 mg, 91% yield).

A portion of the isolated carboxylic acid (50 mg, 0.13 mmol) was dissolved in dichloromethane (1.3 mL), followed by EDC (30 mg, 0.16 mmol), hydroxybenzotriazole (21 mg, 0.16 mmol), and DIEA (338 μL, 0.194 mmol). The solution was allowed to stir at RT 30 min, at which point amine (0.194 mmol) was added. The solution was allowed to stir 16 h under nitrogen atmosphere. The reaction was diluted with additional dichloromethane (20 mL) and then washed with saturated aqueous NH_4Cl solution, H_2O, and brine. The organic layer was dried over $MgSO_4$ and then concentrated in vacuo. Further purification via Biotage silica column (10 g, 100% DCM to 1% MeOH:DCM) afforded the desired compound as a white solid.

*N-Benzyl-1-(4-(4-fluorobenzyl)-4H-thieno[3,2-b]pyrrole-5-carbonyl)piperidine-4-carboxamide (**5a**).* Synthesized from **4a** by procedure A, using benzylamine as the amide coupling partner. TLC R_f (10% MeOH:DCM): 0.45. ^{1}H NMR ($CDCl_3$, 500 MHz): δ (ppm) 7.36 (t, *J* = 6.0 Hz, 2H), 7.33−7.24 (m, 3H), 7.21 (d, *J* = 5.4 Hz, 1H), 7.15 (t, *J* = 5.4 Hz, 2H), 6.97 (t, *J* = 8.7 Hz, 2H), 6.88 (d, *J* = 5.4 Hz, 1H), 6.58 (s, 1H), 5.68 (bs, 1H), 5.44 (s, 2H), 4.54−4.35 (m, 4H), 2.93 (t, *J* = 11.7 Hz, 2H), 2.36 (m, 1H), 1.87−1.79 (m, 2H), 1.61−1.50 (m, 2H). TOF ES+ MS: 476.2 (M + H). HPLC (gradient A): retention time = 7.23, purity >95%.

*N-Benzyl-1-(4-(4-chlorobenzyl)-4H-thieno[3,2-b]pyrrole-5-carbonyl)piperidine-4-carboxamide (**5b**).* Synthesized from **4b** (prepared from **2** as described for **4a** using 4-chlorobenzyl chloride) by procedure A, using benzylamine as the amide coupling partner. TLC R_f (70% EA/hex): 0.2. ^{1}H NMR (400 MHz, DMSO-d_6) δ 8.34(t, *J* = 5.8 Hz,1H), 7.42−7.12 (m, 13H), 6.71 (s, 1H), 5.45 (s, 2H), 4.27 (d, *J* = 5.8 Hz, 4H), 2.93 (m, 1H), 2.42 (m, 1H), 1.71 (d, *J* = 11.2 Hz, 2H), 1.44 (d, *J* = 11.3 Hz, 1H). ^{13}C NMR (400 MHz, DMSO-d_6) 173.5, 161.7, 142.1, 139.5, 137.2, 132.0, 129.5, 129.0, 128.4, 128.1, 127.0, 126.7, 126.6, 121.2, 111.3, 103.9, 48.3, 41.8, 41.5, 28.4. TOF ES + MS: 492.0 (M + H). HPLC (gradient A): retention time = 7.73.

*(S)-1-(4-(4-Fluorobenzyl)-4H-thieno[3,2-b]pyrrole-5-carbonyl)-N-(1-phenylethyl)piperidine-4-carboxamide (**5c**).* Synthesized from **4a** by Procedure A, using (*S*)-α-methylbenzylamine as the amide coupling partner. TLC R_f (1:1 hex:EA): 0.20. ^{1}H NMR ($CDCl_3$, 500 MHz): δ (ppm) 7.37 (t, *J* = 6.0 Hz, 2H), 7.31 (m, 3H), 7.20 (d, *J* = 5.3 Hz, 1H), 7.14 (dd, *J* = 5.3, 8.4 Hz, 2H), 6.96 (t, *J* = 8.7 Hz, 2H), 6.87 (d, *J* = 5.3 Hz, 1H) 6.58 (s, 1H), 5.63 (d, *J* = 7.5 Hz, 1H), 5.43 (s, 2H), 5.15 (quint, *J* = 7.3 Hz, 1H), 4.44 (m, 2H), 2.91 (m, 2H), 2.31 (m, 1H), 1.81 (m, 2H), 1.58 (m, 2H), 1.52 (d, *J* = 6.9 Hz, 3H). TOF ES+ MS: 490.1 (M + H), 512.0 (M + Na). HPLC (gradient A): retention time = 7.47.

*(R)-1-(4-(4-Fluorobenzyl)-4H-thieno[3,2-b]pyrrole-5-carbonyl)-N-(1-phenylethyl)piperidine-4-carboxamide (**5d**).* Synthesized from **4a** by procedure A, using (*R*)-α-methylbenzylamine as the amide coupling partner. TLC R_f (1:1 hex:EA): 0.20. ^{1}H NMR ($CDCl_3$, 500 MHz): δ (ppm) 7.37 (t, *J* = 6.0 Hz, 2H), 7.31 (m, 3H), 7.20 (d, *J* = 5.3 Hz, 1H), 7.14 (dd, *J* = 5.3, 8.4 Hz, 2H), 6.96 (t, *J* = 8.7 Hz, 2H), 6.87 (d, *J* = 5.3 Hz, 1H) 6.58 (s, 1H), 5.63 (d, *J* = 7.5 Hz, 1H), 5.43 (s, 2H), 5.15 (quint, *J* = 7.3 Hz, 1H), 4.44 (m, 2H), 2.91 (m, 2H), 2.31 (m, 1H), 1.81 (m, 2H), 1.58 (m, 2H), 1.52 (d, *J* = 6.9 Hz, 3H). TOF ES+ MS: 490.1 (M + H), 512.1 (M + Na). HPLC (gradient A): retention time = 7.47.

*(R)-N-Benzyl-1-(4-(1-(4-fluorophenyl)ethyl)-4H-thieno[3,2-b]pyrrole-5-carbonyl)piperidine-4-carboxamide (**5e**).* Synthesized from **4e** by procedure A, using benzylamine as the amide coupling partner. TLC R_f (1:1 hex:EA): 0.17. ^{1}H NMR ($CDCl_3$, 500 MHz): δ (ppm) 7.36 (d, *J* = 6.5 Hz, 3H), 7.30 (bm, 4H), 7.09 (d, *J* = 5.2 Hz, 1H), 6.99 (t, *J* = 8.4 Hz, 2H), 6.63 (d, *J* = 5.3 Hz, 1H), 6.55 (s, 1H), 6.02 (quart, *J* = 6.8 Hz, 1H), 5.86 (bs, 1H), 4.52 (m, 2H), 4.47 (s, 2H), 2.96 (m, 2H), 2.38 (quint, *J* = 11.0 Hz, 1H), 1.94 (d, *J* = 6.5 Hz, 3H), 1.89 (m, 2H), 1.63 (m, 2H). TOF ES+ MS: 490.1 (M + H), 512.1 (M + Na). HPLC (gradient A): retention time = 7.50.

*(S)-N-Benzyl-1-(4-(1-(4-fluorophenyl)ethyl)-4H-thieno[3,2-b]pyrrole-5-carbonyl)piperidine-4-carboxamide (**5f**).* Synthesized from **4f** by procedure A, using benzylamine as the amide coupling partner. TLC R_f (1:1 hex:EA): 0.17. ^{1}H NMR ($CDCl_3$, 500 MHz): δ (ppm) 7.36 (d, *J* = 6.5 Hz, 3H), 7.30 (bm, 4H), 7.09 (d, *J* = 5.2 Hz, 1H), 6.99 (t, *J* = 8.4 Hz, 2H), 6.63 (d, *J* = 5.3 Hz, 1H), 6.55 (s, 1H), 6.02 (quart, *J* = 6.8 Hz, 1H), 5.86 (bs, 1H), 4.52 (m, 2H), 4.47 (s, 2H), 2.96 (m, 2H), 2.38 (quint, *J* = 11.0 Hz, 1H), 1.94 (d, *J* = 6.5 Hz, 3H), 1.89 (m, 2H), 1.63 (m, 2H). TOF ES+ MS: 490.1 (M + H), 512.1 (M + Na). HPLC (gradient A): retention time = 7.50.

*Ethyl 1-(4-Chlorobenzyl)-1H-indole-2-carboxylate (**7b**).* Ethyl 1*H*-indole-2-carboxylate **6** (1.50 g, 7.93 mmol) and potassium carbonate (1.42 g, 10.3 mmol) were dissolved in 10 mL of DMF. A 5.0 mL DMF solution of 1-chloro-4-(chloromethyl)benzene (1.66 g, 10.3 mmol) was added. The reaction was placed under nitrogen and heated at 60 °C for 24 h. The reaction was cooled to room temperature and diluted with water (50 mL) and extracted with ethyl acetate (80 mL). The organic layers were combined, washed with saturated sodium chloride solution (100 mL × 3), dried over magnesium sulfate, and concentrated in vacuo to afford a tan solid. Trituration with methanol afforded **7b** as a white solid (1.8 g, 72%). TLC R_f (50% EA/Hex): 0.5. ^{1}H NMR (400 MHz, DMSO-d_6) δ = 7.74 (d, *J* = 8.0 Hz, 1H), 7.59 (d, *J* = 8.5 Hz, 1H), 7.41−7.30 (m, 4H), 7.16 (t, *J* = 7.5 Hz, 1H), 7.04 (d, *J* = 8.3 Hz, 2H), 5.85 (s, 2H), 4.29 (q, *J* = 7.1 Hz, 2H), 1.29 (t, *J* = 7.1 Hz, 3H). TOF ES+ MS: 314.0 (M + H), 336.0 (M + Na). HPLC (gradient A): retention time = 7.88 min.

1-(4-Chlorobenzyl)-1H-indole-2-carboxylic Acid. Compound **7b** and lithium hydroxide (1.53 g, 63.9 mmol) were dissolved in 10 mL of THF and 20 mL of water. The reaction was heated at 60 °C overnight. The reaction was cooled and diluted with water and washed with diethyl ether. The aqueous solution was acidified using 2N HCl acid to pH 2. The resulting suspension was extracted with ethyl acetate. The organic layer was dried over magnesium sulfate, filtered, and concentrated in vacuo to obtain pure product as a white solid (1.47 g, 81%). TLC R_f (50% EA/hex): 0.2. ^{1}H NMR (400 MHz, DMSO-d_6) δ = 13.02 (s, 1H), 7.72 (d, *J* = 8.0 Hz, 1H), 7.54 (d, *J* = 8.5 Hz, 1H), 7.37−7.26 (m, 4H), 7.14 (t, *J* = 7.5 Hz, 1H), 7.05 (d, *J* = 5.6 Hz, 2H), 5.87 (s, 2H). TOF ES+ MS: 286.0 (M + H). HPLC (gradient A): retention time = 7.88 min.

*Ethyl 1-(1-(4-Chlorobenzyl)-1H-indole-2-carbonyl)piperidine-4-carboxylate (**8b**).* 1-(4-Chlorobenzyl)-1*H*-indole-2-carboxylic acid (1.00 g, 3.50 mmol), EDC (1.34 g, 6.99 mmol), and 1-hydroxybenzotriazole (0.946 g, 7.00 mmol) were added to an oven-dried RBF. The solids were dissolved in 4.0 mL of DCM and allowed to stir at room temperature for 15 min. Ethyl piperidine-4-carboxylate (1.08 mL, 7.01 mmol) and DIEA (1.22 mL, 7.00 mmol) were added sequentially. The reaction was allowed to stir overnight at room temperature. The reaction was diluted with water and ethyl acetate. The layers were separated. The ethyl acetate layer was washed with saturated sodium chloride. The organic layer was dried over magnesium sulfate, filtered through a silica gel plug, and concentrated to obtain an oily product. The crude material was triturated in ethyl acetate to obtain white solid as the product (1.29 g, 87%). TLC R_f (60% EA/hex): 0.5. ^{1}H NMR (400 MHz, DMSO-d_6) δ 7.63−7.55 (m, 2H), 7.33−7.28 (m, 2H), 7.22 (t, *J* = 7.1 Hz, 1H), 7.12−7.02 (m, 3H), 6.72 (s, 1H), 5.49 (s, 2H), 4.25 (s, 1H), 4.06 (q, *J* = 7.1, 4.2 Hz, 2H), 3.88 (s, 2H), 2.60−2.52 (m, 1H), 1.75 (s, 2H), 1.44−1.01 (m, 6H). TOF ES+ MS: 286.0 (M + H). HPLC (gradient A): retention time = 7.88 min.

1-(1-(4-Chlorobenzyl)-1H-indole-2-carbonyl)piperidine-4-carboxylic Acid. Compound **8b** (4.2 g, 9.8 mmol) and lithium hydroxide hydrate (4.1 g, 98 mmol) were dissolved in 10 mL of THF and 40 mL of water. The reaction was allowed to stir overnight. The reaction was diluted with water and diethyl ether. The aqueous layer was washed with another aliquot of diethyl ether before it was acidified with 2N HCl to pH ∼ 2. The aqueous layer solution was washed with ethyl acetate (3 × 200 mL). The ethyl acetate layers were combined and washed with saturated aqueous solution of sodium chloride, dried over magnesium sulfate, filtered, and concentrated in vacuo to obtain the product as a white solid (3.33 g, 86%). TLC R_f (60% EA/hex): 0.25. ^{1}H NMR (400 MHz, DMSO-d_6) δ 12.30 (s, 1H), 7.66 (d, *J* = 7.9 Hz, 1H), 7.59 (d, *J* = 8.4 Hz, 1H), 7.35 (d, *J* = 8.4 Hz, 2H), 7.25 (t, *J* = 11.4, 3.9 Hz, 1H), 7.16−7.09 (m, 3H), 6.75 (s, 1H), 5.52 (s, 2H), 4.29 (s, 1H), 4.04 (s, 1H), 3.06 (s, 2H), 2.52−2.47 (m, 1H), 1.80 (s, 2H), 1.22 (s, 2H). TOF ES+ MS: (M + H). HPLC (gradient A): retention time = 6.98 min.

General Procedure B for Preparing Compounds 9a−m. 1-(1-(4-Chlorobenzyl)-1*H*-indole-2-carbonyl)piperidine-4-carboxylic acid (1.0 equiv), EDC (2.0 equiv), and 1-hydroxybenzotriazole (2.0 equiv) were dissolved in DCM (3.0 mL) and allowed to stir at room temperature for 15 min. DIEA (2.0 equiv) and desired amine (2.0 equiv) were added. The reaction was allowed to stir at room temperature overnight. The reaction was diluted with water and ethyl acetate. The organic layer was washed with water, saturated sodium bicarbonate, 1N HCl, and saturated sodium chloride. The organic layer was dried over magnesium sulfate, filtered, and concentrated in vacuo. The crude material was recrystallized in diethyl ether/ethyl acetate to afford desired product.

*N-Benzyl-1-(1-(4-fluorobenzyl)-1H-indole-2-carbonyl)piperidine-4-carboxamide (**9a**).* Synthesized from **6** as described for **9b** using 4-fluorobenzyl chloride instead of 4-chlorobenzyl chloride. Flash chromatography with 0−5% methanolic ammonia: DCM afforded CCG 203880 as a white solid (60 mg, 48%). TLC R_f (5% methanolic ammonia/DCM): 0.2. ^{1}H NMR (400 MHz, DMSO-d_6) δ 8.33 (t, *J* = 5.8 Hz, 1H), 7.60 (dd, *J* = 16.0, 8.2 Hz, 2H), 7.35−7.06 (m, 11H), 6.72 (s, 1H), 5.48 (s, 2H), 4.44 (bs, 1H), 4.27 (d, *J* = 5.7 Hz, 2H), 4.03 (bs, 1H), 2.91 (bs, 2H), 2.47−2.40 (m, 1H), 1.78 (bs, 2H), 1.45 (bs, 2H). TOF ES+ MS: 470.1 (M + H), 492.1 (M + Na). HPLC (gradient A): retention time = 7.77 min.

*N-Benzyl-1-(1-(4-chlorobenzyl)-1H-indole-2-carbonyl)piperidine-4-carboxamide (**9b**).* Prepared by procedure B using benzylamine. TLC R_f (70% EA/hex): 0.2. ^{1}H NMR (400 MHz, DMSO-d_6) δ 8.35 (t, *J* = 5.9 Hz, 1H0, 7.63 (d, *J* = 7.9 Hz, 1H), 7.55 (d, *J* = 8.3 Hz, 1H), 7.38−7.29 (m, 4H), 7.27−7.29 (m, 4H), 7.27−7.18 (m, 4H), 7.14−7.08 (m, 3H), 6.74 (s, 1H), 5.50(s, 2H), 4.43 (bs, 1H), 4.28 (d, *J* = 5.9 Hz, 2H), 4.04 (bs, 1H), 2.95 (bs, 2H), 2.48−2.42 (m, 2H), 1.74 (bs, 2H), 1.47 (bs, 2H). ^{13}C NMR (500 MHz, DMSO-d_6) 173.4, 161.8, 139.5, 137.1, 136.7, 131.7, 126.1, 123.0, 121.3, 120.1, 110.6, 103.30.

dx.doi.org/10.1021/jm300214e | J. Med. Chem. 2012, 55, 3535−3545

TOF ES+ MS: 486.1 (M + H), 508.0 (M + Na). HPLC (gradient A): retention time = 7.73 min.

*1-(1-(4-Chlorobenzyl)-1H-indole-2-carbonyl)-N-phenylpiperidine-4-carboxamide (**9d**).* Synthesized according to procedure B using aniline. White solid (77 mg, 65%). TLC R_f (70% EA/hex): 0.2. ^{1}H NMR (400 MHz, DMSO-d_6) δ 9.89 (s, 1H), 7.66−7.52 (m, 4H), 7.37−7.18 (m, 5H), 7.13−7.07 (m, 3H), 7.02 (t, J = 7.4 Hz, 1H), 6.75 (s, 1H), 5.51(s, 2H), 4.45 (bs, 1H), 4.03 (bs, 1H), 2.95 (bs, 2H), 2.64−2.55 (m, 1H), 1.79 (bs, 2H), 1.47 (bs, 2H). TOF ES+ MS: 472.1 (M + H), 494.1 (M + Na). HPLC (gradient A): retention time = 8.01 min.

*1-(1-(4-Chlorobenzyl)-1H-indole-2-carbonyl)-N-phenethylpiperidine-4-carboxamide (**9e**).* Synthesized according to procedure B using 2-phenethylamine. White solid (76 mg, 60%). TLC R_f (70% EA/hex): 0.2. ^{1}H NMR (400 MHz, DMSO-d_6) δ 7.85 (t, J = 5.4 Hz, 1H), 7.62 (d, J = 7.8 Hz, 1H), 7.53 (d, J = 8.4 Hz, 1H), 7.36−7.05 (m, 10H), 6.71 (s, 1H), 5.48 (s, 2H), 4.38 (bs, 1H), 4.01 (bs, 1H), 3.26 (q, J = 13.6, 6.7 Hz, 2H), 2.90 (bs, 2H), 2.69 (t, J = 13.6, 6.5 Hz, 2H), 2.39−2,28 (m, 2H), 1.61 (bs, 2H), 1.36 (bs, 2H). TOF ES+ MS: 500.2 (M + H), 522.1 (M + Na). HPLC (gradient A): retention time = 7.90 min.

*1-(1-(4-Chlorobenzyl)-1H-indole-2-carbonyl)-N-(4-methylphenethyl)piperidine-4-carboxamide (**9f**).* Synthesized according to procedure B using *p*-methyl phenethylamine. Flash chromatography with 0−5% methanolic ammonia/DCM afforded **9f** as a white solid (24 mg, 19%). TLC R_f (0−5% methanolic ammonia/DCM): 0.25. ^{1}H NMR (400 MHz, DMSO-d_6). δ 7.86 (t, J = 5.5 Hz, 1H), 7.64 (d, J = 8.0 Hz, 1H), 7.56 (d, J = 8.3 Hz, 1H), 7.35 (d, J = 8.4 Hz, 2H), 7.23 (t, J = 7.6 Hz, 1H), 7.14−7.03 (m, 7H), 6.73 (s, 1H), 5.50 (s, 2H), 4.40 (bs, 1H), 3.91 (bs, 1H), 3.24 (q, J = 12.0, 6.3 Hz, 2H), 2.90 (bs, 2H), 2.66 (t, J = 7.3 Hz, 2H), 2.40−2.30 (m, 1H), 2.27 (s, 3H), 1.65 (bs, 2H), 1.36 (bs, 2H). TOF ES+ MS: 514.1 (M + H), 536.1 (M + Na). HPLC (gradient A): retention time = 8.15 min.

*(S)-1-(1-(4-Chlorobenzyl)-1H-indole-2-carbonyl)-N-(1-phenylethyl)piperidine-4-carboxamide (**9g**).* Synthesized according to procedure B using (*S*)-1-phenylethylamine. White solid (32.9 mg, 26%). TLC R_f (70% EA/hex): 0.2. ^{1}H NMR (400 MHz, DMSO-d_6) δ 8.25 (d, J = 8.0 Hz, 1H), 7.62 (d, J = 7.9 Hz, 1H), 7.53 (d, J = 8.4 Hz, 1H), 7.35−7.25 (m, 5H), 7.21 (t, J = 7.3 Hz, 2H), 7.09 (d, J = 7.7 Hz, 3H), 6.72 (s, 1H), 5.48 (s, 2H), 4.97−4.82 (m, 1H), 4.42 (bs, 1H), 4.03 (bs, 1H), 2.89 (bs, 2H), 2.46−2.39 (m, 1H), 1.68 (bs, 2H), 1.52−1.26 (m, 5H). ^{13}C NMR (400 MHz, DMSO-d_6) 172.6, 161.8, 144.8, 137.1, 136.7, 131.8, 131.7, 128.7, 128.3, 128.1, 126.4, 126.1, 125.7, 123.0, 121.3, 120.1, 110.6, 103.3, 47.4, 46.1, 41.4, 22.4. TOF ES+ MS: 500.0 (M + H), 522.1 (M + Na). HPLC (gradient A): retention time = 7.88 min. [CHN] C = 71.8%, H = 6.07%, N = 8.37%. Theoretical [CHN]: C = 72.06%, 6.05%, 8.4%.

*(R)-1-(1-(4-Chlorobenzyl)-1H-indole-2-carbonyl)-N-(1-phenylethyl)piperidine-4-carboxamide (**9h**).* Synthesized according to procedure B using (*R*)-1-phenylethylamine. White solid (282 mg, 45%). TLC R_f (70% EA/hex): 0.2. ^{1}H NMR (400 MHz, DMSO-d_6) δ 8.25 (d, J = 8.1 Hz, 1H), 7.62 (d, J = 7.9 Hz, 1H), 7.53 (d, J = 8.3 Hz, 1H), 7.36−7.26 (m, 6H), 7.21 (t, J = 7.4 Hz, 2H), 7.10 (d, J = 8.2 Hz, 3H), 6.72 (s, 1H), 5.48 (s, 2H), 4.90 (p, J = 7.1 Hz, 1H), 4.41 (bs, 1H), 4.03 (bs, 1H), 2.89 (bs, 2H), 2.47−2.38 (m, 1H), 1.69 (bs, 2H), 1.52−1.25 (m, 5H). ^{13}C NMR (400 MHz, DMSO-d_6) 172.6, 161.8, 144.7, 137.1, 136.7, 131.8, 131.7, 128.7, 128.3, 128.1, 126.4, 126.1, 125.7, 123.0, 121.3, 120.1, 110.6, 103.3, 47.4, 46.1, 41.4, 22.4. TOF ES + MS: 500 (M + H), 522.1 (M + Na). HPLC (gradient A): retention time = 7.87 min. [CHN] C = 71.93%, H = 6.06%, N = 8.39%. Theoretical [CHN]: C = 72.06%, 6.05%, 8.4%.

*1-(1-(4-Chlorobenzyl)-1H-indole-2-carbonyl)-N-(4-methoxybenzyl)piperidine-4-carboxamide (**9i**).* Synthesized according to procedure B using 4-methoxybenzylamine. Trituration in methanol afforded **9i** as white solid (104 mg, 80%). TLC R_f (70% EA/hex): 0.2. ^{1}H NMR (400 MHz, DMSO-d_6). δ 8.25 (t, J = 5.8 Hz, 1H), 7.57 (dd, J = 34.9, 8.1 Hz, 2H), 7.33 (d, J = 8.4 Hz, 2H), 7.20 (t, J = 7.7 Hz, 1H), 7.11 (m, 4H), 6.86 (d, J = 8.6 Hz, 2H), 6.72 (s, 1H), 5.48 (s, 2H), 4.43 (s, 1H), 4.18 (d, J = 5.8 Hz, 2H), 4.01 (s, 1H), 3.71 (s, 3H), 2.93 (s, 2H), 2.41 (d, J = 11.7 Hz, 1H), 1.70 (s, 2H), 1.42 (s, 2H). TOF ES+ MS: 516.1 (M + H), 538.1 (M + Na). HPLC (gradient A): retention time = 8.27 min; purity = 91%.

*N-(3-Chlorobenzyl)-1-(1-(4-chlorobenzyl)-1H-indole-2-carbonyl)-piperidine-4-carboxamide (**9j**).* Synthesized according to procedure B using 3-chlorobenzylamine. Trituration in methanol afforded afforded **9j** as a white solid (179 mg, 49%). TLC R_f (70% EA/hex): 0.3. ^{1}H NMR (400 MHz, DMSO-d_6). δ 8.40 (t, J = 6.0 Hz, 1H), 7.63 (d, J = 8.0 Hz, 1H), 7.54 (d, J = 8.3 Hz, 1H), 7.38−7.06 (m, 14H), 6.73 (1H), 5.49 (s, 2H), 4.45 (bs, 1H) 4.27 (d, J = 5.6 Hz, 2H), 4.08 (bs, 1H), 2.94 (bs, 2H), 2.48−2.43 (m, 1H), 1.77 (bs, 2H), 1.40 (bs, 2H). TOF ES+ MS: 520.0 (M + H). HPLC (gradient A): retention time = 8.06 min.

*(1-(4-Chlorobenzyl)-1H-indol-2-yl)(4-(piperidine-1-carbonyl)-piperidin-1-yl)methanone (**9k**).* Synthesized according to procedure B using piperidine. Flash chromatography with 0−5% methanolic ammonia/DCM afforded **9k** as a white solid (48 mg, 41%). TLC R_f (0−5% methanolic ammonia/DCM): 0.2. ^{1}H NMR (400 MHz, DMSO-d_6) δ 7.62 (d, J = 7.8 Hz, 1H), 7.54 (d, J = 8.3 Hz, 1H), 7.33 (d, J = 8.5 Hz, 2H), 7.21 (t, J = 11.8, 4.6 Hz, 1H), 7.13−7.07 (m, 3H), 6.73 (s, 1H), 5.49 (s, 2H), 4.44 (bs, 1H), 4.02 (bs, 1H), 3.43 (s, 4H), 3.20−3.83 (m, 3H), 1.79−1.20 (m, 10H). TOF ES+ MS: 464.1 (M + H), 486.1 (M + Na). HPLC (gradient A): retention time = 7.95 min.

*1-(1-(4-Chlorobenzyl)-1H-indole-2-carbonyl)-N-(pyridin-4-ylmethyl)piperidine-4-carboxamide (**9l**).* Synthesized according to procedure B using 4-aminomethyl pyridine to afford **9l** as a white solid (61 mg, 50%). TLC R_f (100% EA): 0.1. ^{1}H NMR (400 MHz, DMSO-d_6). δ 8.68−8.59 (m, 4H), 7.63 (d, J = 7.8 Hz, 1H), 7.54 (d, J = 8.4 Hz, 1H), 7.49 (d, J = 5.9 Hz, 4H), 7.36−7.30 (m, 3H), 7.22 (t, J = 7.6 Hz, 1H), 7.14−7.07 (m, 2H), 6.74 (s, 1H), 5.49 (s, 2H), 4.56−4.14 (m, 4H), 2.97 (bs, 2H), 1.76 (bs, 2H), 1.43 (bs, 2H). TOF ES+ MS: 487.1 (M + H). HPLC (gradient A): retention time = 8.00 min.

*1-(1-(4-Chlorobenzyl)-1H-indole-2-carbonyl)-N-(pyridin-3-ylmethyl)piperidine-4-carboxamide (**9m**).* Synthesized according to procedure B using 3-aminomethyl pyridine to afford **9m** as a white solid (315 mg, 70%). TLC R_f (100% EA): 0.1. ^{1}H NMR (400 MHz, DMSO-d_6). δ 8.46 (d, J = 8.3 Hz, 1H), 8.40(t, J = 5.7 Hz, 1H), 7.70−7.60 (m, 1H), 7.54 (d, J = 8.3 Hz, 1H), 7.40−7.29 (m, 1H), 7.21 (t, J = 7.6 Hz, 1H), 7.13−7.05 (m, 1H), 6.73 (s, 1H), 5.49 (s, 1H), 4.38 (bs, 1H), 4.30 (d, J = 5.8 Hz, 2H), 4.04 (bs, 1H), 2.95 (bs, 2H), 2.47−2.41 (m, 1H), 1.72 (bs, 2H), 1.41 (bs, 2H). TOF ES+ MS: 487.1 (M + H). HPLC (gradient A): retention time = 5.62 min.

Ethyl 1-(1-(4-Chlorobenzyl)-1H-indole-2-carbonyl)piperidine-3-carboxylate. Compound **7b** (100 mg, 0.319 mmol), EDC (134 mg, 0.699 mmol) and 1-hydroxybenzotriazole (95.0 mg, 0.703 mmol) were dissolved in DCM (volume: 3.0 mL). The reaction was allowed to stir for 10 min before the addition of DIEA (0.122 mL, 0.700 mmol) and ethyl piperidine-3-carboxylate (0.109 mL, 0.707 mmol). The reaction was allowed to stir overnight at room temperature. The reaction was diluted with water and ethyl acetate. The organic phase was washed with water, 1N HCl, saturated sodium bicarbonate, and saturated sodium chloride. The organic layer was dried over magnesium sulfate, filtered, and concentrated in vacuo. The crude material was purified using Biotage SP1 system with 0−45% ethyl acetate/hexanes to afford white solid. (100 mg, 67%) TLC R_f (60% EA/hex): 0.5. ^{1}H NMR (400 MHz, DMSO-d_6). δ 7.63 (d, J = 7.9 Hz, 1H), 7.55 (d, J = 8.3 Hz, 1H), 7.33 (d, J = 8.4 Hz, 2H), 7.22 (t, J = 7.3 Hz, 1H), 7.16−7.06 (m, 3H), 6.73 (s, 1H), 5.46 (s, 2H), 4.47−3.63 (m, 5H), 3.29−2.70 (m, 2H), 1.94−1.03 (m, 4H). TOF ES+ MS: 425.1(M + H), 447.1 (M + Na). HPLC (gradient A): retention time = 8.36 min.

1-(1-(4-Chlorobenzyl)-1H-indole-2-carbonyl)piperidine-3-carboxylic Acid. Ethyl 1-(1-(4-chlorobenzyl)-1*H*-indole-2-carbonyl)-piperidine-3-carboxylate (100 mg, 0.235 mmol) and solid lithium hydroxide (99 mg, 2.4 mmol) were dissolved in 1.5 mL of THF and 3.0 mL of water. The reaction was allowed to stir overnight. After 24 h at room temperature, the reaction was diluted with water and extracted twice with diethyl ether. The aqueous layer was acidified with 2N HCl aqueous solution to pH 2 and extracted with three times with ethyl acetate. The organic layers were combined and washed with saturated sodium chloride solution, dried over magnesium sulfate, filtered, and concentrated in vacuo to obtain a white solid. The crude material was taken directly to the next step without further purification. (50 mg, 53%) TLC R_f (60% EA/hex): 0.2. ^{1}H NMR (400 MHz, DMSO-d_6) δ = 12.26 (s, 1H), 7.63 (d, J = 7.9 Hz, 1H), 7.54 (d, J = 8.4 Hz, 1H),

7.33 (d, J = 8.4 Hz, 2H), 7.22 (t, J = 7.6 Hz, 1H), 7.16−7.04 (m, 3H) 6.73 (s, 1H), 5.46 (s, 2H), 4.21 (s, 1H), 3.94 (s, 1H), 3.02 (s, 2H), 1.99 (s, 1H), 1.96−1.52 (m, 2H), 1.40−0.97 (m, 2H). TOF E+ MS: 397.1 (M + H), 419.1 (M + Na). HPLC (gradient A): retention time = 6.98 min.

*N-Benzyl-1-(1-(4-chlorobenzyl)-1H-indole-2-carbonyl)piperidine-3-carboxamide (**9c**).* Synthesized according to procedure B using 1-(1-(4-chlorobenzyl)-1*H*-indole-2-carbonyl)piperidine-3-carboxylic acid and benzylamine. Flash chromatography with 0−5% methanolic ammonia: DCM afforded **9c** as a white solid (38 mg, 62%). TLC R_f (70% EA/hex): 0.2. ^{1}H NMR (400 MHz, DMSO-d_6). δ 8.44 (s, 1H), 7.60 (d, J = 7.9 Hz, 1H), 7.49 (s, 1H), 7.36−7.03 (m, 12H), 6.72 (s, 1H), 5.46 (s, 2H), 4.58−3.74 (m, 4H), 2.93 (bs, 2H), 2.30 (s, 1H), 1.93−1.48 (m, 3H). TOF ES+ MS: 486.1 (M + H), 508.1 (M + Na). HPLC (gradient A): retention time = 7.99 min.

Mouse Liver Microsome (MLM) Stability Assay. Balb-C mouse liver microsomes (MLM) were purchased from Invitrogen. $MgCl_2$ and NADPH were obtained from Sigma. Solvents were of HPLC grade or better. The HPLC-MS/MS system consisted of a ThermoElectron Finnigan TSQ Quantum Ultra AM.

Microsomal incubations were done in triplicate. Incubation mixtures contained 2 μL of 20 mg/mL microsomes (approximately 0.04 mg microsomal protein), 4 μL of 100 mM DMSO-dissolved substrate (1.0 μM final), in 475 μL potassium phosphate buffer (0.1 M, pH 7.5, containing 3.3 mM $MgCl_2$.) The incubation mixture was allowed to shake at 37 °C for 5 min, and a T = 0 aliquot was removed. Reaction was initiated by the addition of 20 μL of NADPH (22 mM under the same buffer conditions), and the mixture was allowed to shake at 37 °C until the final aliquot was removed. Then 30 μL aliquots were taken after 0, 5, and 15 min. All aliquots were quenched by dilution in 90 μL of MeCN containing an internal standard, and the precipitate was pelleted via centrifugation. Then 20 μL of supernatant was injected onto the HPLC-MS/MS. Mobile phase A was 95:5 H_2O/MeCN with 0.1% formic acid, and mobile phase B was MeCN with 0.1% formic acid. Column used was a Luna C18(2) 4.6 mm × 30 mm column with 3 μM particle size. The flow rate was 2 mL/min, and a gradient mobile phase composition was used: isocratic hold for 1 min at 90% A (10% B), 1 min gradient to 10% A (90% B), 1 min gradient back to 90% A (10% B), and 1 min isocratic hold at 90% A (10% B). Ionization method consisted of positive electrospray. Source parameters were optimized for each individual substrate. Substrates and internal standards were followed by selected reaction monitoring. Substrate/internal standard area ratios were determined and converted into percent substrate remaining. The natural log of the percent remaining was plotted against time, the slope of the linear regression was determined, and the equation $T_{1/2} = -\ln(2)/k$ was used to calculate half-life. $T_{1/2}$ values cited in the manuscript are means of $N \geq 3$ experiments.

Parallel Artificial Membrane Permeability Assay (PAMPA). Compounds were dissolved in DMSO to generate a 10 mM compound solution. The experiment was performed using the Double-Sink protocol provided by pION, Inc. with the PAMPA Explorer system. A cosolvent system solution was used for the experiment.

In Vitro Antiviral and Cytotoxicity Assays. The WEEV replicon assay was done as previously described[12] with the following modifications. We obtained a clonal derivative of the original BSR-T7 cell line by limiting dilution and used this clonal cell line for all replicon assays. The BSR-T7/C3 clone was cultured in Dulbecco's Modified Eagle Medium containing 5% heat inactivated fetal bovine serum, 1% sodium pyruvate, 0.1 mM non-essential amino acids, 10 U/mL penicillin, and 10 μg/mL streptomycin. Cells were cultured in the above media with 0.5 mg/mL G418 every third passage to maintain selection. Cells were transfected in 10 cm tissue culture plates for 2 h, detached by trypsinization, and transferred to 96-well plates preloaded with compound dilutions. Final cell concentrations were ~2 × 10^6 cells/mL, and plates were harvested 18−20 h later for luciferase and MTT assays as previously described.[12] BE(2)-C cell culture, virus infections, and plaque assays were done as previously described.[23] Cells were infected with WEEV or NSV at a multiplicities of infection of 0.1 or 10, respectively, to obtain approximately 20−25% residual cell viability at 24 h post-infection.

Induction of Experimental Viral Encephalitis. Female C57BL/6 mice were purchased from The Jackson Laboratory (Bar Harbor, ME). All animals were housed and used on-site under specific pathogen-free conditions in strict accordance with guidelines set by the National Institutes of Health and protocols approved by the University Committee on the Use and Care of Animals. Mice were housed on a 10/14 h light/dark cycle in ventilated cages containing no more than five animals per cage. Food and water were available ad libitum.

To induce encephalomyelitis, 5−6-week-old mice were anesthetized with isoflurane (Abbott Laboratories, Chicago, IL) and 1000 plaque-forming units (PFU) of the prototype alphavirus, neuroadapted Sindbis virus (NSV), suspended in 10 μL of phosphate-buffered saline (PBS) were inoculated directly into the right cerebral hemisphere of each animal. Experimental antiviral compounds were solubilized in dimethyl sulfoxide (DMSO) as stock solutions (100 μM) and then diluted in PBS to generate working solutions for intraperitoneal injection into infected mice on a twice-daily dosing schedule. For those experiments where clinical outcome was the primary end point, each infected mouse was scored daily into one of the following categories: (1) normal, (2) mild paralysis (some weakness of one or both hind limbs), (3) moderate paralysis (weakness of one hind limb, paralysis of the other hind limb), (4) severe paralysis (complete paralysis of both hind limbs), or (5) dead. Other groups of animals were sacrificed at defined intervals post-infection in order to collect brain and spinal cord tissue for ex vivo analysis. Following intracardiac perfusion with ice-cold PBS, the left cerebral hemisphere and lower spinal cord was isolated from some animals, snap-frozen on dry ice, and stored at −80 °C for virus titration assays (see below). Alternatively, naïve or NSV-infected mice were sequentially perfused with ice-cold PBS and then chilled 4% paraformaldehyde (PFA) in PBS so that the brains and spinal cords could be removed intact for histopathological analyses (see below).

Virus Titration Assays. Homogenates (10% w/v) of each tissue sample were prepared in PBS, and serial 10-fold dilutions of each homogenate were assayed for plaque formation on monolayers of BHK-21 cells, as previously described.[24] Results are presented as the geometric mean ± standard error of the mean (SEM) of the $\log_{10}$ number of PFU per gram of tissue derived from four animals at each time point.

Histopathology Analyses. Nervous system tissues were post-fixed overnight at 4 °C in 4% PFA. The axonal processes of motor neurons (MN) in the lumbar spinal cord that innervate the hind limb musculature were quantified in cross sections of ventral spinal nerve roots as a correlate of hind limb paralysis according to published methods.[25,26] All experimental samples were collected from mice 14 days post-infection because the loss of MN axons is delayed following destruction of the cell body within the spinal cord itself. Sections of the lumbar spinal column at the L4−L5 level were decalcified (Immunocal, Decal Corporation, Tallman, NY) and embedded in paraffin. Sections were then stained using a modified Bielchowsky silver staining method to label the neurofilament proteins of each nerve axon.[25−29] Axonal density (the number of intact axons per cross-sectional area of each nerve root) was determined for the right and left L4 and L5 ventral nerve roots from a minimum of four animals in each experimental group.

Neuronal damage in the brain was assessed in cryosections through the hippocampal formations of naïve and day 14 NSV-infected mice. Virus consistently and prominently infects this brain region.[20] Before staining, each section was incubated in 0.1% Triton X-100 for 15 min to expose intracellular antigens. Slides were then incubated with NisslRed (NeuroTrace 530/615 fluorescent Nissl stain, Invitrogen, Grand Island, NY) diluted 1:100 for 20 min, washed, incubated in a 0.06% potassium permanganate solution, washed again, and stained in 0.0001% Fluoro-Jade C compound (Millipore, Billerica, MA) in 1% acetic acid for 10 min. After further washing, slides were dried, dehydrated in xylene, and coverslipped using VectaMount permanent mounting media (Vector Laboratories, Burlingame, CA). The right and left hippocampi from each animal were imaged at 20× magnification using a Nikon Ti−U

inverted fluorescence microscope supported by the NIS-Elements Basic Research acquisition and analysis software (Nikon Instruments Inc., Melville, NY). The total number of Fluoro-Jade-positive/NisslRed-positive cells (degenerating neurons) and NisslRed-positive cells (all neurons) was counted in duplicate slides from each hippocampus of triplicate mice for each experimental condition to determine the proportion of Fluoro-Jade-positive neurons.

Statistical Analyses. The Prism 5.0 software package (GraphPad Software, La Jolla, CA) was used for all statistical analyses. Differences in severity of paralysis and survival among cohorts of infected mice were measured using a log-rank (Mantel−Cox) test. Unpaired Student's *t* test was used to assess differences between tissue viral titers or neuronal counts between two experimental groups at single time points. In all cases, differences at a $p < 0.05$ level were considered significant.

AUTHOR INFORMATION

Corresponding Author

*For S.D.L.: phone, 734 615 0454; E-mail, sdlarsen@umich.edu. For D.J.M.: phone, 734 763 0565; E-mail, milldavi@umich.edu.

Author Contributions

#S.D.L. and D.J.M. contributed equally to this work.

Notes

The authors declare no competing financial interest.

ACKNOWLEDGMENTS

This work was supported by an NIH Partnerships for Biodefense Viral Pathogens grant (R01 AI089417), an NIH Pharmacological Sciences Training Program fellowship for B.D.Y. (T32 GM007767), and a UM Rackham Merit Scholarship for S.J.B. We thank Dr. Brian Shay for assistance with the LC/MS/MS analysis of samples from the MLM stability assays.

ABBREVIATIONS USED

CNS, central nervous system; CPE, cytopathic effect; HTS, high-throughput screen; EDC, *N*-(3-dimethylaminopropyl)-*N*′-ethylcarbodiimide hydrochloride; MTT, 3-(4,5-dimethylthiazol-2-yl)-2,5-diphenyltetrazolium bromide; NSV, neuroadapted Sindbis virus; VEEV, Venezuelan equine encephalitis virus; WEEV, western equine encephalitis virus; PAMPA, parallel artificial membrane permeability assay; MLM, mouse liver microsome

REFERENCES

(1) Gubler, D. J. The global emergence/resurgence of arboviral diseases as public health problems. *Arch. Med. Res.* **2002**, *33* (4), 330−342.

(2) Nash, D.; Mostashari, F.; Fine, A.; Miller, J.; O'Leary, D.; Murray, K.; Huang, A.; Rosenberg, A.; Greenberg, A.; Sherman, M.; Wong, S.; Layton, M. The outbreak of West Nile virus infection in the New York City area in 1999. *N. Engl. J. Med.* **2001**, *344* (24), 1807−1814.

(3) Soldan, S. S.; Gonzalez-Scarano, F. Emerging infectious diseases: the Bunyaviridae. *J. Neurovirol.* **2005**, *11* (5), 412−423.

(4) Enserink, M. Infectious diseases. Chikungunya: no longer a third world disease. *Science* **2007**, *318* (5858), 1860−1861.

(5) *NIAID Biodefense Research Agenda for Category B and C Priority Pathogens*. Available at: http://www.niaid.nih.gov/topics/BiodefenseRelated/Biodefense/Documents/categorybandc.pdf, January 2003.

(6) Sidwell, R. W.; Smee, D. F. Viruses of the Bunya- and Togaviridae families: potential as bioterrorism agents and means of control. *Antiviral Res.* **2003**, *57* (1−2), 101−111.

(7) Bronze, M. S.; Huycke, M. M.; Machado, L. J.; Voskuhl, G. W.; Greenfield, R. A. Viral agents as biological weapons and agents of bioterrorism. *Am. J. Med. Sci.* **2002**, *323* (6), 316−325.

(8) Puig-Basagoiti, F.; Tilgner, M.; Forshey, B. M.; Philpott, S. M.; Espina, N. G.; Wentworth, D. E.; Goebel, S. J.; Masters, P. S.; Falgout, B.; Ren, P.; Ferguson, D. M.; Shi, P. Y. Triaryl pyrazoline compound inhibits flavivirus RNA replication. *Antimicrob. Agents Chemother.* **2006**, *50* (4), 1320−1329.

(9) Pohjala, L.; Alakurtti, S.; Ahola, T.; Yli-Kauhaluoma, J.; Tammela, P. Betulin-derived compounds as inhibitors of alphavirus replication. *J. Nat. Prod.* **2009**, *72* (11), 1917−1926.

(10) Pohjala, L.; Barai, V.; Azhayev, A.; Lapinjoki, S.; Ahola, T. A luciferase-based screening method for inhibitors of alphavirus replication applied to nucleoside analogues. *Antiviral Res.* **2008**, *78* (3), 215−222.

(11) Pohjala, L.; Utt, A.; Varjak, M.; Lulla, A.; Merits, A.; Ahola, T.; Tammela, P., Inhibitors of alphavirus entry and replication identified with a stable Chikungunya replicon cell line and virus-based assays. *PLoS One 6* (12), e28923.

(12) Peng, W.; Peltier, D. C.; Larsen, M. J.; Kirchhoff, P. D.; Larsen, S. D.; Neubig, R. R.; Miller, D. J. Identification of thieno[3,2-*b*]pyrrole derivatives as novel small molecule inhibitors of neurotropic alphaviruses. *J. Infect. Dis.* **2009**, *199* (7), 950−957.

(13) Venable, J. D.; Cai, H.; Chai, W.; Dvorak, C. A.; Grice, C. A.; Jablonowski, J. A.; Shah, C. R.; Kwok, A. K.; Ly, K. S.; Pio, B.; Wei, J.; Desai, P. J.; Jiang, W.; Nguyen, S.; Ling, P.; Wilson, S. J.; Dunford, P. J.; Thurmond, R. L.; Lovenberg, T. W.; Karlsson, L.; Carruthers, N. I.; Edwards, J. P. Preparation and biological evaluation of indole, benzimidazole, and thienopyrrole piperazine carboxamides: potent human histamine h(4) antagonists. *J. Med. Chem.* **2005**, *48* (26), 8289−8298.

(14) Blair, J. B.; Marona-Lewicka, D.; Kanthasamy, A.; Lucaites, V. L.; Nelson, D. L.; Nichols, D. E. Thieno[3,2-*b*]- and thieno[2,3-*b*]pyrrole bioisosteric analogues of the hallucinogen and serotonin agonist *N*,*N*-dimethyltryptamine. *J. Med. Chem.* **1999**, *42* (6), 1106−1111.

(15) Bonafoux, D.; Abibi, A.; Bettencourt, B.; Burchat, A.; Ericsson, A.; Harris, C. M.; Kebede, T.; Morytko, M.; McPherson, M.; Wallace, G.; Wu, X., Thienopyrrole acetic acids as antagonists of the CRTH2 receptor. *Bioorg. Med. Chem. Lett. 21* (6), 1861-1864.

(16) Golantsov, N.; Karchava, A.; Starikova, Z.; Dolgushin, F.; Yurovskaya, M. Chirally *N*-Substituted Indole-2-carbaldehydes. Preparation and Use in Asymmetric Synthesis. *Chem. Heterocycl. Compd.* **2005**, *41* (10), 1290−1299.

(17) Lipinski, C. A.; Lombardo, F.; Dominy, B. W.; Feeney, P. J. Experimental and computational approaches to estimate solubility and permeability in drug discovery and development settings. *Adv. Drug Delivery Rev.* **1997**, *23* (1−3), 3−25.

(18) Kansy, M.; Avdeef, A.; Fischer, H. Advances in screening for membrane permeability: high-resolution PAMPA for medicinal chemists. *Drug Discovery Today* **2004**, *1*, 349−355.

(19) Jackson, A. C.; Moench, T. R.; Griffin, D. E.; Johnson, R. T. The pathogenesis of spinal cord involvement in the encephalomyelitis of mice caused by neuroadapted Sindbis virus infection. *Lab. Invest.* **1987**, *56* (4), 418−423.

(20) Jackson, A. C.; Moench, T. R.; Trapp, B. D.; Griffin, D. E. Basis of neurovirulence in Sindbis virus encephalomyelitis of mice. *Lab. Invest.* **1988**, *58* (5), 503−509.

(21) Li, Y.; Wang, L.; Li, S.; Chen, X.; Shen, Y.; Zhang, Z.; He, H.; Xu, W.; Shu, Y.; Liang, G.; Fang, R.; Hao, X. *seco*-Pregnane steroids target the subgenomic RNA of alphavirus-like RNA viruses. *Proc. Natl. Acad. Sci. U.S.A.* **2007**, *104* (19), 8083−8088.

(22) Julander, J. G.; Bowen, R. A.; Rao, J. R.; Day, C.; Shafer, K.; Smee, D. F.; Morrey, J. D.; Chu, C. K. Treatment of Venezuelan equine encephalitis virus infection with (−)-carbodine. *Antiviral Res.* **2008**, *80* (3), 309−315.

(23) Castorena, K. M.; Peltier, D. C.; Peng, W.; Miller, D. J. Maturation-dependent responses of human neuronal cells to western equine encephalitis virus infection and type I interferons. *Virology* **2008**, *372* (1), 208−220.

(24) Irani, D. N.; Prow, N. A. Neuroprotective interventions targeting detrimental host immune responses protect mice from fatal alphavirus encephalitis. *J. Neuropathol. Exp. Neurol.* **2007**, *66* (6), 533−544.
(25) Havert, M. B.; Schofield, B.; Griffin, D. E.; Irani, D. N. Activation of divergent neuronal cell death pathways in different target cell populations during neuroadapted sindbis virus infection of mice. *J. Virol.* **2000**, *74* (11), 5352−5356.
(26) Prow, N. A.; Irani, D. N. The opioid receptor antagonist, naloxone, protects spinal motor neurons in a murine model of alphavirus encephalomyelitis. *Exp. Neurol.* **2007**, *205* (2), 461−470.
(27) Kerr, D. A.; Larsen, T.; Cook, S. H.; Fannjiang, Y. R.; Choi, E.; Griffin, D. E.; Hardwick, J. M.; Irani, D. N. BCL-2 and BAX protect adult mice from lethal Sindbis virus infection but do not protect spinal cord motor neurons or prevent paralysis. *J. Virol.* **2002**, *76* (20), 10393−10400.
(28) Nargi-Aizenman, J. L.; Havert, M. B.; Zhang, M.; Irani, D. N.; Rothstein, J. D.; Griffin, D. E. Glutamate receptor antagonists protect from virus-induced neural degeneration. *Ann. Neurol.* **2004**, *55* (4), 541−549.
(29) Prow, N. A.; Irani, D. N. The inflammatory cytokine, interleukin-1 beta, mediates loss of astroglial glutamate transport and drives excitotoxic motor neuron injury in the spinal cord during acute viral encephalomyelitis. *J. Neurochem.* **2008**, *105* (4), 1276−1286.